AIP | Journal of Applied Physics

Edge effects on the electronic properties of phosphorene nanoribbons

Xihong Peng, Andrew Copple, and Qun Wei

Citation: Journal of Applied Physics **116**, 144301 (2014); doi: 10.1063/1.4897461
View online: http://dx.doi.org/10.1063/1.4897461
View Table of Contents: http://scitation.aip.org/content/aip/journal/jap/116/14?ver=pdfcov
Published by the AIP Publishing

Edge effects on the electronic properties of phosphorene nanoribbons

Xihong Peng,[1,a)] Andrew Copple,[2] and Qun Wei[1,3]
[1]*School of Letters and Sciences, Arizona State University, Mesa, Arizona 85212, USA*
[2]*Department of Physics, Arizona State University, Tempe, Arizona 85287, USA*
[3]*School of Physics and Optoelectronic Engineering, Xidian University, Xi'an 710071, People's Republic of China*

(Received 24 July 2014; accepted 27 September 2014; published online 8 October 2014)

Two dimensional few-layer black phosphorus crystal structures have recently been fabricated and have demonstrated great potential in electronic applications. In this work, we employed first principles density functional theory calculations to study the edge and quantum confinement effects on the electronic properties of the phosphorene nanoribbons (PNR). Different edge functionalization groups, such as H, F, Cl, OH, O, S, and Se, in addition to a pristine case were studied for a series of ribbon widths up to 3.5 nm. It was found that the armchair-PNRs (APNRs) are semiconductors for all edge groups considered in this work. However, the zigzag-PNRs (ZPNRs) show either semiconductor or metallic behavior in dependence on their edge chemical species. Family 1 edges (i.e., H, F, Cl, OH) form saturated bonds with P atoms in the APNRs and ZPNRs, and the edge states keep far away from the band gap. However, Family 2 edges (pristine, O, S, Se) form weak unsaturated bonds with the p_z orbital of the phosphorus atoms and bring edge states within the band gap of the ribbons. For the ZPNRs, the edge states of Family 2 are present around the Fermi level within the band gap, which close up the band gap of the ZPNRs. For the APNRs, these edge states are located at the bottom of the conduction band and result in a reduced band gap. © *2014 AIP Publishing LLC*. [http://dx.doi.org/10.1063/1.4897461]

I. INTRODUCTION

Recently, fabricated two dimension (2D) few-layer black phosphorus[1–4] has drawn immediate attention to the society of material science.[5–16] This material is chemically inert and has promising transport properties. It has carrier mobility up to 1000 $cm^2/V{\cdot}s$ and an on/off ratio up to 10^4 was achieved for the phosphorene transistors at room temperature.[1,2] In addition, this material shows a finite direct band gap at the Γ point of the Brillouin zone[1,2,5,7,17,18] (in contrast to the vanishing gap in 2D graphene sheet), which creates potential for additional applications in optoelectronics.

Tailoring electronic properties of semiconductors has been critical for applications in electronics. A series of strategies were explored to engineer the band gap of phosphorene, for example, by utilizing multilayer structures,[1,5] applying mechanical strains,[6,7] forming nanoribbons[9,12–14] or nanotubes.[9] For the phosphorene nanoribbons (PNRs), their electronic properties are dependent on the crystal orientation of the ribbons. For example, two typical crystal directions were generally explored, namely the armchair-PNRs (APNRs) and the zigzag-PNRs (ZPNRs). Tran and Yang[12] reported that the PNRs with the edge phosphorus atoms passivated using H are direct-gap semiconductors and their band gaps are a strong function of the ribbon width due to the quantum confinement effect. However, Guo *et al.*[9] found that the pristine ZPNRs are metals regardless of the ribbon width, while the pristine APNRs are semiconductors with indirect band gaps. These distinct conclusions imply that the edges of the ribbons play a critical role on their electronic properties. Therefore, it is important to systematically study the edge effects on the PNRs, in particular, with several common chemical groups, such as -OH, -O, -S. In this work, we present detailed systematic analysis of the edge effects on the electronic band structure and density of states (DOS) of both APNRs and ZPNRs for a series of ribbon widths up to 3.5 nm. Our results suggest that the APNRs are semiconductors with either direct or indirect band gap depending on the edge functionalization groups, and the ZPNRs demonstrate either semiconductor or metallic behavior with different edge passivation.

II. CALCULATION DETAILS

The theoretical calculations were carried out using first principles density functional theory (DFT).[19] The Perdew-Burke-Ernzerhof (PBE) exchange-correlation functional[20] and the projector-augmented wave (PAW) potentials[21,22] were employed. The calculations were performed using the Vienna Ab-initio Simulation Package (VASP).[23,24] The kinetic energy cutoff for the plane wave basis set was chosen to be 500 eV. The energy convergence criteria for electronic and ionic iterations were set to be 10^{-5} eV and 10^{-4} eV, respectively. The reciprocal space was meshed at $14 \times 1 \times 1$ for the ZPNRs and $1 \times 10 \times 1$ for the APNRs using Monkhorst Pack meshes centered at Γ point. 21 K-points were included in band structure calculations from Γ to X for the ZPNRs and from Γ to Y for the APNRs. To simulate a ribbon, a unit cell with periodic boundary condition was used. A vacuum space of at least 20 Å was

[a)]Author to whom correspondence should be addressed. Electronic mail: xihong.peng@asu.edu.

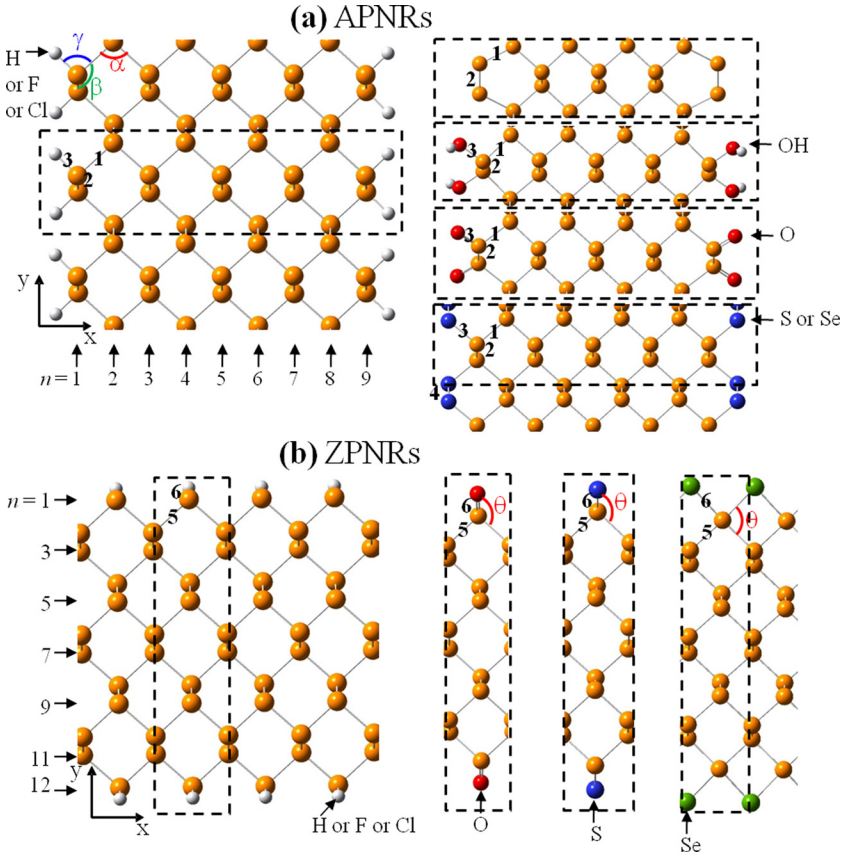

FIG. 1. Snapshots of the APNRs and ZPNRs with different edge functionalization groups. (a) 9L-APNR with edge P atoms saturated using H (F or Cl), and hydroxyl group, double-bonded O, and bridge-bonded S (Se) atoms, respectively. (b) 12L-ZPNR with edge functionalized using H (F or Cl), double-bonded O, S and bridge-bonded Se atoms, respectively. The dashed rectangles indicate the unit cells.

included in the unit cell to minimize the interaction between the system and its replicas resulting from the periodic boundary condition.

III. RESULTS AND DISCUSSIONS

A. Structural properties

The initial structures of monolayer phosphorene were obtained from bulk black phosphorus.[25] The 2D phosphorene has a puckered honeycomb structure with each phosphorus atom covalently bonded with three adjacent atoms. Our calculated lattice constants for bulk black phosphorus are $a = 3.307$ Å, $b = 4.547$ Å, and $c = 11.210$ Å, in good agreement with experimental values[25] and other theoretical calculations.[1,26] The relaxed lattice constants for monolayer phosphorene are $a = 3.295$ Å and $b = 4.618$ Å.

The APNRs and ZPNRs with different ribbon widths up to 3.5 nm were truncated from monolayer phosphorene along the y- and x-directions, respectively, as shown in Figure 1. The width of a ribbon nL is referring to the number n of P atoms in the direction perpendicular to the ribbon direction (see Figure 1). As an example, Figure 1 demonstrates the snapshots of 9L-APNRs and 12L-ZPNRs. The edges of the PNRs were treated in eight different scenarios: no passivation (pristine) or bonded with H, F, Cl, OH, O, S, or Se chemical species.

We explored the structural configuration at the edges for the PNRs. For example, six bond lengths labeled as b1–b6 and four bond angles indicated as α, β, γ, and θ in Figure 1 were calculated and reported in Table I. There is negligible change in the bond length b1 (between the two P atoms near the edge of the 9L-APNR) for all eight different edge groups, indicating that the distinct edge functionalization groups only affect the geometry on the very edge of the ribbons. The P-P bond b2 on the very edge for the pristine case experiences a considerable reduction from 2.26 Å (of the 2D phosphorene) to 2.07 Å, due to its edge dangling-bond reconstruction. The variation in the bond length b3 between the P atoms and the edge species is expected: larger edge chemical species yields a longer bond length. The bond b3 is sufficiently large for the edge S (Se) case, such that two S (Se) atoms in the neighbored simulation cell form a bond, labeled

TABLE I. The bond lengths b1-b6 and bond angles α-θ at the edges of the PNRs with different edge chemical groups. The bond lengths and angles were denoted in Figure 1. As a reference, the corresponding bond lengths/angles in monolayer phosphorene were also listed.

	9L-APNR							12L-ZPNR		
System	b1 (Å)	b2 (Å)	b3 (Å)	b4 (Å)	α (°)	β (°)	γ (°)	b5 (Å)	b6 (Å)	θ (°)
Monolayer	2.22	2.26	n/a	n/a	95.9	104.1	n/a	2.22	n/a	104.1
Pristine	2.23	2.07	n/a	n/a	111.1	119.1	n/a	2.14	n/a	n/a
H	2.22	2.25	1.44	n/a	95.7	103.2	93.1	2.23	1.44	99.3
F	2.23	2.25	1.63	n/a	94.9	98.3	98.3	2.22	1.64	106.0
Cl	2.24	2.26	2.08	n/a	92.7	95.9	101.1	2.23	2.08	107.3
OH	2.23	2.24	1.68	n/a	94.9	99.0	100.1	2.22	1.68	110.7
O	2.27	2.25	1.49	n/a	99.5	106.7	109.2	2.25	1.50	116.4
S	2.23	2.25	2.11	2.10	97.0	105.0	99.5	2.28	2.00	106.3
Se	2.23	2.24	2.28	2.38	95.3	102.9	100.0	2.29	2.39	89.3

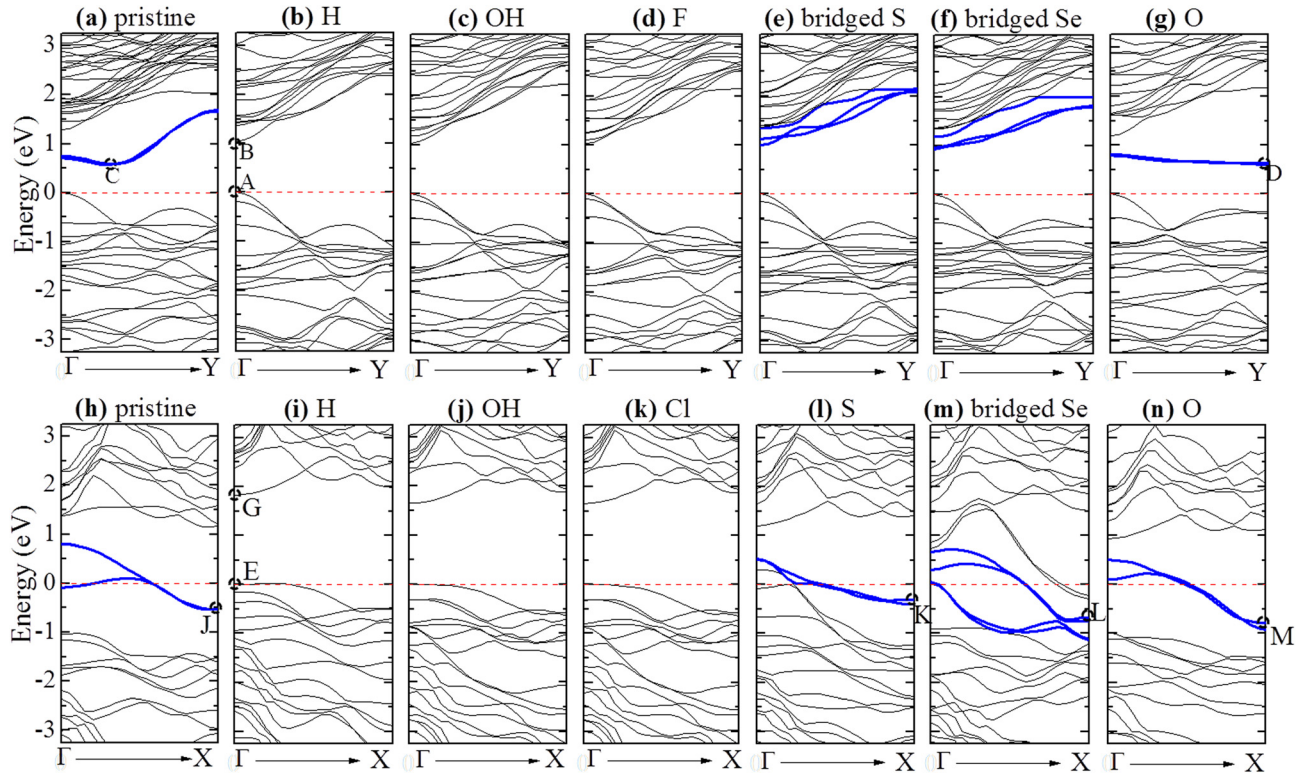

FIG. 2. Band structures of the APNRs and ZPNRs with different edge chemical groups. Top is for the 9L-APNRs and Bottom for the 12L-ZPNR. The Fermi level is aligned at zero. The states brought by the edge P, O, S, and Se atoms within the band gap are indicated in blue color.

as b4 in Figure 1(a). The bond angles α and β both increase largely for the pristine case due to the reconstruction of the edge P-P bond.

For the ZPNRs, the bond lengths b5 and b6 show similar variations with the edge functionalization groups as the b2 and b3 in the APNRs, respectively. The significantly reduced bond angle θ in the Se case from 104.1° (of the 2D phosphorene) to 89.3° results from the special bridge-bonding configuration as shown in Figure 1(b). We also checked this bridge-bonding arrangement for both O and S edges and found that these two species prefer to bond to one P atom rather than the bridge-bond to two P atoms, as shown in Figure 1(b). This gives much shorter bond length b6, 1.50 Å and 2.00 Å for the O and S cases, respectively, comparing to 2.39 Å in the Se edge.

B. Band structure and density of states

The band structures of the PNRs with the eight different edge functionalization groups were calculated. As an example, Figure 2 presents the band structures of the 9L-APNRs and 12L-ZPNRs. Since the edge groups F and Cl show similar effects on the band structure, we only plot the F-edge case for the APNR and the Cl case for the ZPNR in Figure 2. It is clear that the APNR is a semiconductor. The band gap is defined as the energy difference between the conduction band minimum (CMB) and valence band maximum (VBM). For the pristine and O-edge cases, the APNR shows an indirect band gap, while other functionalization groups demonstrate a direct band gap. For the pristine and O-edge cases, the CBM, which is contributed from the edge P and O atoms, respectively (Figure 4), is not located at the Γ point, while the VBM is at Γ, which gives an indirect gap. However, for the cases with the edge H, OH, F(Cl), both the CBM and VBM are contributed by the non-edge P atoms (i.e., intrinsic states) in the ribbon and located at Γ, which gives a direct band gap. A slightly different situation occurs for the APNRs with the edge S (Se) atoms, in which the conduction bands are mainly contributed by the edge S (Se), while the CBM is still located at Γ and results in a direct band gap.

On the other hand, the ZPNR shows a dissimilar behavior. The ribbon demonstrates either semiconductor or metallic behavior as shown in Figures 2(h)–2(n), in dependence on the edge functionalization groups. The edge chemical groups can be classified into two distinct families. Family 1 includes the H, OH, F, and Cl edges and Family 2 consists of the pristine, O, S, and Se cases. For Family 1 edges, the ZPNRs are semiconductors with a direct band gap at Γ. Their CBM and VBM are the intrinsic states from the non-edge P atoms in the ribbon (Figure 4). However, for Family 2 edges, the ribbon shows metallic behavior. The electronic states contributed by the edge atoms are located around the Fermi level and close up the band gap.

The DOS of the studied PNRs was also calculated. As an example, Figure 3 presents the total, s- and p-orbital projected DOS of the 9L-APNRs and 12L-ZPNRs. The DOS of the 9L-APNR with the edge S (O) passivation in Figure 3 suggests that the ribbons are semiconductors, in which the conduction band (CB) was mainly contributed by the p-orbitals of the edge P and S (O) atoms, while the VBM is located at the p-

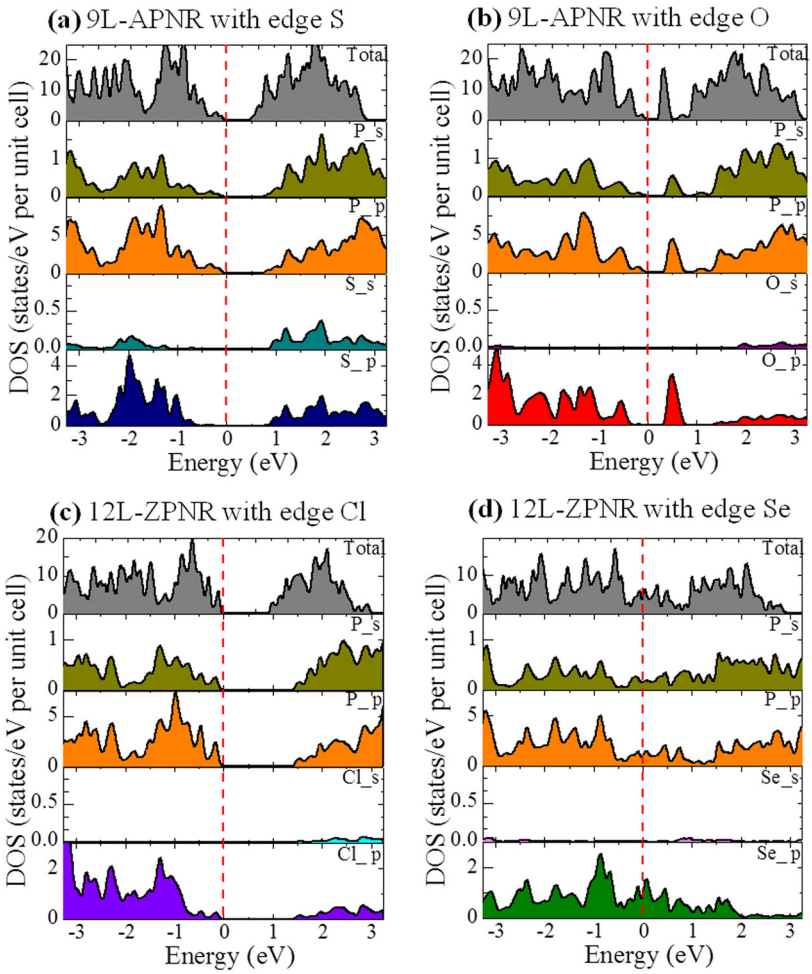

FIG. 3. The total, s- and p-orbital projected density of states. The DOS of the 9L-APNR with the edge functionalized using (a) S and (b) O atoms. The DOS of the 12L-ZPNR with the edge saturated using (c) Cl and (d) bridge-bonded Se atoms. The Fermi level is aligned at zero.

orbitals of the P atoms in the ribbons. For the 12L-ZPNR with the edge Cl in Figure 3(c), the band gap of the ribbon is determined by the intrinsic states of P and the Cl states being far away from the band gap. In the metallic 12L-ZPNR with the bridge-bonded Se in Figure 3(d), the p-orbitals of the Se and P atoms form bonds which close up the gap.

The near-band-edge states A–M (labeled in Figure 2) were explored and their electron density contour plots are presented in Figure 4. States A and B are the VBM and CBM of the 9L-APNR with the edge H atoms. The wave function of states A and B are primarily located in the phosphorus atoms within the ribbon and the edge P and H atoms have little contribution. It was found that State A and B also represent the VBM and CBM of the 9L-APNR with other edges in Family 1 (i.e., F, Cl, and OH). State C is the CBM of the pristine 9L-APNR. From the electron density contour plot in Figure 4(c), it is clear that the charge is primarily located at the edge P atoms. State D is the CBM of the 9L-APNR with the edge O and the charge is distributed mainly on the edge P and O atoms. Similar edge states within the band gap were also found for the S and Se cases.

In the 12L-ZPNRs, the electronic states E and G are denoted as the VBM and CBM with the edge H atoms and they are intrinsic states contributed by the non-edge P atoms. It was found that the VBM and CBM with other Family 1 edges are the same State E and G, respectively. However, for the pristine, S, Se, and O cases (Family 2), the charges of

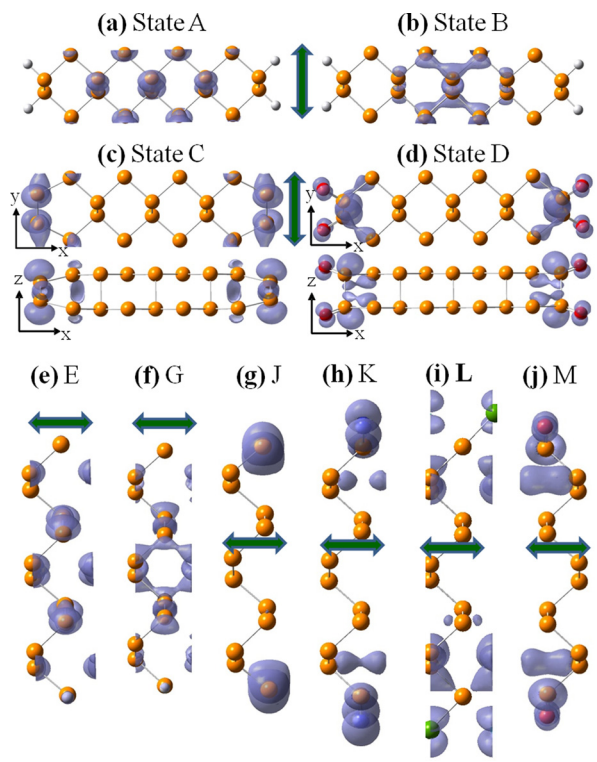

FIG. 4. The electron density contour plots of near-Fermi-level states A–M. The vertical and horizontal arrows indicate the armchair and zigzag ribbon directions (periodic boundary), respectively.

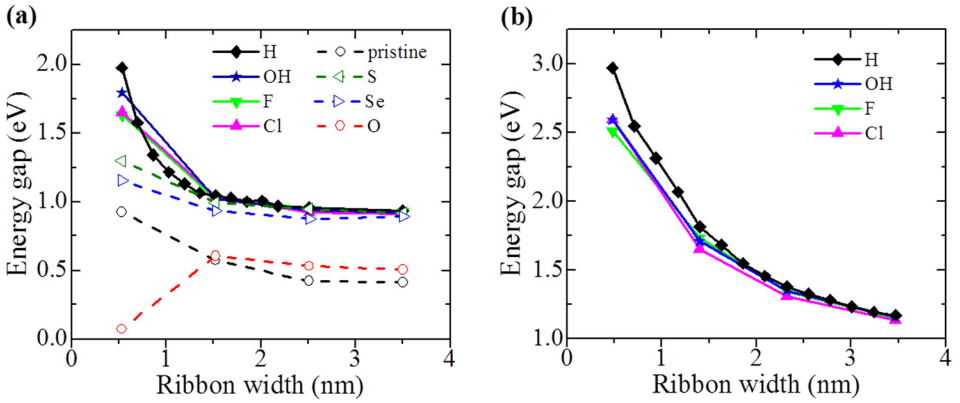

FIG. 5. The band gap of the (a) APNRs and (b) ZPNRs as a function of ribbon width. Family 1 edges are plotted using solid lines while Family 2 edges are denoted with dashed lines.

states J, K, L, and M are primarily located on the edge P and chemical groups.

To understand why Family 2 structures bring edge states within the band gap while Family 1 edges do not, we examined the characteristics of the electronic orbitals of the near-gap states. Family 1 edge species form a saturated bond with the P atoms and the energy associated with this saturated bond is far below the Fermi level. For example, the energy associated with the P-F bond in the 9L-APNR is 4.12 eV below the Fermi energy and that of the P-O bond in the case of edge OH group is 2.09 eV below the Fermi level. However, in Family 2 cases, the P atoms do not form a saturated bond with the edge species. Moreover, these unsaturated bonds are particularly weak due to their special electronic orbital orientations. For instance, the edge reconstructed P-P bond in the pristine ribbon is nearly in the ribbon plane (i.e., the xy-plane). However, the p-orbitals of the two P atoms are along the z-direction (i.e., p_z-orbital). And the p_z-orbitals form a relatively weak P-P bond in the xy-plane due to a minimal overlap of the wavefunction. A similar situation was found for the O, S, and Se cases. For example, in Figure 4(d), the p_z-orbitals of the edge O and P atoms cause a weak P-O bond in the ribbon plane (i.e., the xy-plane). These weak unsaturated bonds bring the edge states within the band gap for Family 2 cases. It is interesting to note that the bridge-bonded Se atoms in the ZPNR appear to form a saturated bond with two P atoms. However, their p_z-orbitals make these P-Se-P bonds in the ribbon plane relatively weak, and such weak bonds brings edge states within the band gap to close the gap.

C. Quantum confinement on band gaps

The band gap of the APNRs and semiconducting ZPNRs with the ribbon width up to 3.5 nm were calculated and presented in Figure 5. For the APNRs in Figure 5(a), the band gap of Family 1 cases increases rapidly with reducing width of the ribbon. Note from the above discussion, the band gap of Family 1 is determined by the intrinsic electronic states of phosphorus atoms. The scaling of the band gap with the ribbon width d obeys the usual $1/d^2$ relation according to quantum confinement, which is consistent with literature.[12] Given the same ribbon width, the band gap of Family 2 ribbons is generally smaller than that of Family 1. This is because Family 2 cases bring edge states within the band gap, thus largely reducing the gap. The significantly smaller band gap of the 3L-APNR with the edge O results from a structural distortion of this ultra narrow ribbon. For the ZPNRs in Figure 5(b), the four Family 1 ribbons have very similar behavior, and the gap scaled as $1/d$, in agreement with Tran and Yang's prediction.[12] Family 2 ZPNRs show metallic behavior, thus the gap is zero.

IV. CONCLUSIONS

In summary, we employed first principles DFT calculations to study electronic properties of the phosphorene nanoribbons with the edge functionalization using different chemical groups. It was found that the APNRs are semiconductors for all edge groups considered in this work. However, the ZPNRs demonstrate either semiconducting or metallic behavior. The CBM and VBM of the APNRs and ZPNRs with the edge H, F, Cl, and OH groups (Family 1 edges) are contributed by the intrinsic electronic states of non-edge phosphorus atoms, and the edge species have negligible contribution to the wavefunctions of the CBM and VBM. Therefore, the ribbons in this family are semiconductors with a direct band gap. However, the APNRs and ZPNRs in the pristine, O, S, and Se cases (Family 2 edges) display edge states within the band gap, which cause a reduced band gap in the APNRs and metallic behavior in the ZPNRs. These edge states in Family 2 ribbons originate from their weak unsaturated bond with the P atoms.

ACKNOWLEDGMENTS

This work was supported by the Faculty Research Fund from School of Letters and Sciences at Arizona State University (ASU) to Peng. The authors thank ASU Advanced Computing Center and XSEDE for providing computing resources. Dr. F. Tang is acknowledged for the helpful discussions and critical review of the manuscript.

[1]H. Liu, A. T. Neal, Z. Zhu, Z. Luo, X. Xu, D. Tománek, and P. D. Ye, Acs Nano **8**(4), 4033–4041 (2014).
[2]L. Li, Y. Yu, G. Jun Ye, Q. Ge, X. Ou, H. Wu, D. Feng, X. Hui Chen, and Y. Zhang, Nat. Nanotechnol. **9**, 372–377 (2014).
[3]F. Xia, H. Wang, and Y. Jia, Nature Commun. **5**, 4458 (2014).
[4]E. S. Reich, Nature **506**, 19 (2014).
[5]V. Tran, R. Soklaski, Y. Liang, and L. Yang, Phys. Rev. B **89**, 235319 (2014).
[6]R. Fei and L. Yang, Nano Lett. **14**(5), 2884–2889 (2014).
[7]X. Peng, A. Copple, and Q. Wei, Phys. Rev. B **90**, 085402 (2014).
[8]J. Dai and X. C. Zeng, J. Phys. Chem. Lett. **5**(7), 1289–1293 (2014).

[9]H. Guo, N. Lu, J. Dai, X. Wu, and X. C. Zeng, J. Phys. Chem. C **118**(25), 14051–14059 (2014).
[10]Q. Wei and X. Peng, Appl. Phys. Lett. **104**, 251915 (2014).
[11]W. Lu, H. Nan, J. Hong, Y. Chen, C. Zhu, Z. Liang, X. Ma, Z. Ni, C. Jin, and Z. Zhang, Nano Res. **7**(6), 853–859 (2014).
[12]V. Tran and L. Yang, Phys. Rev. B **89**, 245407 (2014).
[13]A. Maity, A. Singh, and P. Sen, e-print arXiv:1404.2469.
[14]A. Carvalho, A. S. Rodin, and A. H. C. Neto, e-print arXiv:1404.5115.
[15]H. Y. Lv, W. J. Lu, D. F. Shao, and Y. P. Sun, e-print arXiv:1404.5171.
[16]M. Buscema, D. J. Groenendijk, S. I. Blanter, G. A. Steele, H. S. J. van der Zant, and A. Castellanos-Gomez, Nano Lett. **14**(6), 3347 (2014).
[17]Y. Takao and A. Morita, Physica B & C **105**(1–3), 93–98 (1981).
[18]A. S. Rodin, A. Carvalho, and A. H. Castro Neto, Phys. Rev. Lett. **112**, 176801 (2014).
[19]W. Kohn and L. J. Sham, Phys. Rev. **140**(4A), A1133–A1138 (1965).
[20]J. P. Perdew, K. Burke, and M. Ernzerhof, Phys. Rev. Lett. **77**(18), 3865–3868 (1996).
[21]P. E. Blochl, Phys. Rev. B **50**(24), 17953–17979 (1994).
[22]G. Kresse and D. Joubert, Phys. Rev. B **59**(3), 1758–1775 (1999).
[23]G. Kresse and J. Furthmuller, Phys. Rev. B **54**(16), 11169 (1996).
[24]G. Kresse and J. Furthmuller, Comput. Mater. Sci. **6**(1), 15–50 (1996).
[25]A. Brown and S. Rundqvist, Acta Cryst. **19**, 684 (1965).
[26]J. Qiao, X. Kong, Z.-X. Hu, F. Yang, and W. Ji, Nat. Commun. **5**, 4475 (2014).